

Shapes of Polyelectrolyte Titration Curves. 2. The Deviant Behavior of Labile Polyelectrolytes

Yuguo Cui,[†] Robert Pelton,^{*,‡} and Howard Ketelson[‡]

McMaster Centre for Pulp and Paper Research, Department of Chemical Engineering, JHE-136, McMaster University, Hamilton, Ontario, Canada, L8S 4L7, and Alcon Laboratories, Fort Worth, Texas 76134

Received May 22, 2008; Revised Manuscript Received September 5, 2008

ABSTRACT: Hydroxypropyl guar (HPG), a nonionic water soluble polymer, becomes an anionic polyelectrolyte in the presence of borate or boronate ions which bind to HPG. However, the charge groups on the HPG–borate are labile which complicates the interpretation of polyelectrolyte titration behavior. Specifically, polyelectrolyte complex formation between HPG–borate and cationic poly(diallyldimethyl ammonium chloride), PDADMAC, stimulates further borate binding to HPG. We propose that labile polyelectrolytes such as HPG–borate are new class of polyelectrolytes that fall outside conventional “strong” or “weak” polyelectrolyte behavior.

Introduction

Polyelectrolyte titrations, originally called the colloid titration,¹ are widely used to measure the concentration of charged groups bound to polymer chains and solid surfaces in water. This technique is based on the quantitative, irreversible complex formation between oppositely charged polyelectrolytes.² Originally, polyelectrolyte titration end points were detected with an indicator dye. However, the streaming current detector (SCD) is widely used for end point detection. The SCD consists of a loosely fitting fluorocarbon coated piston that reciprocates in a cylinder with a closed end (see Figure 1). Electrodes measure the streaming current induced by the flow of liquid over the cylinder walls. It is assumed that polyelectrolyte complex species in solution are identical to those adsorbed on the SCD cylinder wall so that the SCD signal gives a measure of the electrostatic potential of the polyelectrolyte complex species in solution. For example, the curve labeled PVSK, potassium poly(vinyl sulfate), in Figure 2 shows the evolution of SCD signal with addition of PDADMAC, poly(diallyldimethyl ammonium chloride), to a PVSK solution. This is the behavior of classic, well-behaved polyelectrolytes; there are similar examples in the literature.^{3–6} Because of the dramatic change in signal near the equivalence point, most practitioners simply assign an end point corresponding to an SCD signal of 0 mV and do not report the entire titration curve.

In this paper, we present and interpret the colloid titration curves of deviant systems we call “labile polyelectrolytes”; the curve labeled HPG–borate in Figure 2 is an example. The HPG–borate curve in Figure 2 refers to titration of a mixture of hydroxypropyl guar (HPG) and sodium borate. HPG is a water-soluble, nonionic polymer that binds borate ions giving the structure of HPG shown in Figure 3. The hydroxypropyl groups are added to guar to inhibit intermolecular interactions and thus improve water solubility.⁷ The distribution hydroxypropyl groups is approximately random.⁸ A single borate ion can condense onto two HPG segments to give a cross-link, increasing viscosity and giving gels.⁹ Audebert emphasized that, in addition to cross-linking, borate addition converts nonionic guar (or HPG) into an anionic polyelectrolyte.¹⁰

The goal of this paper is to explain the shape of the HPG–borate curve, including identifying the location and

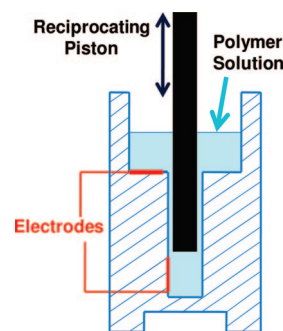


Figure 1. Schematic illustration of a streaming current detector.

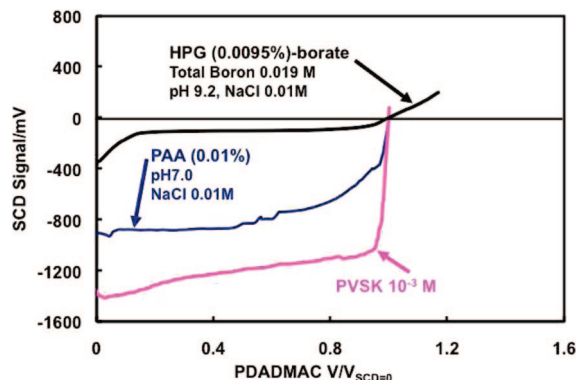


Figure 2. Comparison of polyelectrolyte titration curves for PVSK, a strong polyelectrolyte, PAA a weak polyelectrolyte, and HPG–borate, a labile polyelectrolyte.

meaning of the end point. From an analytical chemistry perspective, the unusual behavior of HPG–borate titration is important because we will show that the end point does not correspond to zero SCD signal, and that the end point is not a measure of the initial charge content of HPG–borate. From a polyelectrolyte physical chemistry perspective, this work is also significant because it suggests a new class of polyelectrolytes – “labile polyelectrolytes”, which display more complicated behaviors. The properties of HPG–borate are now described in context with classic “strong” and “weak” polyelectrolytes.

It is common practice to divide polyelectrolytes into “strong” and “weak”. Strong polyelectrolytes bear charge groups such as sulfate, sulfonate and quaternary ammonium, whose degrees of ionization are not sensitive to pH and ionic strength. By

* Corresponding author. Telephone: (905) 529 7070 ext. 27045. Fax: (905) 528 5114. E-mail: peltonrh@mcmaster.ca.

[†] McMaster Centre for Pulp and Paper Research, Department of Chemical Engineering, JHE-136, McMaster University.

[‡] Alcon Laboratories.

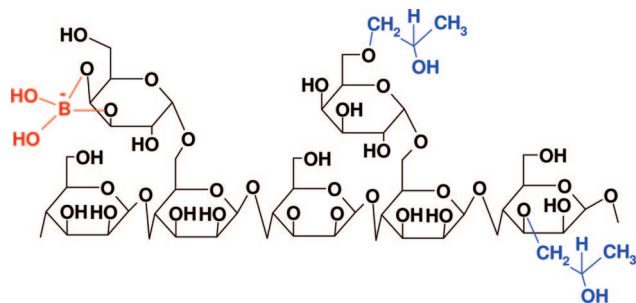


Figure 3. The structure of HPG–borate.

contrast, with weak polyelectrolytes such as polyvinylamine¹¹ and poly(acrylic acid), the degree of ionization is very sensitive to pH and ionic strength. It is generally accepted that borate $B(OH)_4^-$, and not $B(OH)_3$, binds to HPG because alkaline pH is required to observe viscosity increases and other measures of borate binding. This pH sensitivity suggests HPG–borate is another “weak polyelectrolyte”, however, such a conclusion is misleading. Borate–guar binding constants in the literature are 11 L/mol¹⁰ and 100 L/mol.¹² By contrast, the free energy associated with the protonation of poly(acrylic acid) is about 5 times greater than the borate binding energy.¹³

In this paper we explain the unusual polyelectrolyte titration behavior of HPG–borate, and related systems, as a manifestation of the low borate binding constant to HPG. Future work will show that this labile polyelectrolyte characteristic also impacts interactions with cationic surfactants.

Experimental Section

Hydroxypropyl guar (HPG) with 0.36 hydroxypropyl groups per sugar ring and molecular weight of 1.0×10^6 Da was a gift from Alcon Laboratories, Fort Worth Texas. Poly(diallyldimethylammonium chloride), (PDADMAC) solutions (1 meq/L) with molecular weight of 10 700 Da and potassium polyvinyl sulfate (PVSK) (1 meq/L) with molecular weight of 19 100 Da were purchased from BTG Americas Inc. Poly(acrylic acid) with molecular weight of 1.0×10^6 Da was purchased from Polysciences Inc. Methylboronic acid was purchased from Sigma-Aldrich. Sodium borate (borax), sodium hydroxide and hydrochloric acid were purchased from Anachemia. Sodium chloride was purchased from Caledon Laboratories Inc. All experiments were performed with water from a Millipore MilliQ system.

Polyelectrolyte titrations were performed using a Mutek PCD T3 titrator fitted with a Mutek PCD 03 streaming current detector (SCD). The heart of the detector is a reciprocating piston fitted in a fluoropolymer cylinder (see Figure 1). In a typical experiment, 42 mL of 0.01% HPG and 2.1 mL of 0.1 M borax solutions were mixed and the pH was adjusted with sodium hydroxide or hydrochloric acid solution. Ionic strengths of the solutions were adjusted with sodium chloride. A 10 mL sample was loaded into the cell, and was allowed to equilibrate for 30 min before starting the titration. The mixture was titrated with 1 mequiv/L PDADMAC. The apparatus automatically added 0.02–0.2 mL increments of PDADMAC, and the SCD signal was recorded when the drift rate was below 8 mV in 10 s. All experiments were performed at room temperature.

The pH change during addition of PDADMAC to HPG–borate solutions was measured with a Thermo pH electrode connected to a Beckman $\Phi 390$ pH/Temp/mV/ISE Meter. In a typical experiment, 42 mL of 0.01% HPG and 0.01–0.05 mL of 0.1 M sodium borate were added to a 100 mL beaker. PDADMAC (1 meq/L) was manually titrated to HPG and borax solutions under stirring and pH was recorded after each addition.

Modeling Polyelectrolyte Titrations. The goal of this section is to present a model that simulates the range of titration curves shown in Figure 2. Because SCD detectors are commercial devices, we do not know the detailed nature of the SCD signal. Following

Walker’s approach we assume that the SCD signal is proportional to the zeta potential (ζ) of the SCD wall.¹⁴ Furthermore, we assume that the proportionality factor α is a constant for a titration.

$$\text{SCD signal} = \alpha \zeta \quad (1)$$

Initially in a titration, the SCD cell contains a dilute solution of anionic polyelectrolyte that adsorbs onto the SCD fluorocarbon wall, influencing the ζ potential and the net surface charge density, σ_{dl} . For the case of strong polyelectrolyte pairs, such as PVSK titrated with PDADMAC, we assumed that the net charge density changed linearly with the volume of added PDADMAC, V_T —see eq 2, where β is a constant.

$$\sigma_d = \sigma_{dl} + \beta V_T \quad (2)$$

Our previous publication focused only on the strong polyelectrolyte titration case and we showed that classical diffuse double layer theory could be used to simulate the evolution of the SCD signal during a colloid titration.² According to standard diffuse double layer theory, the corresponding net charge density, σ_d , on the SCD cell wall is given by eq 3, where N_A is Avogadro’s number, k is the Boltzmann constant, T is temperature, ϵ is the combined dielectric constant and c is the sodium chloride molarity. Equations 2 and 3 can simulate the shapes of polyelectrolyte titrations with strong polyelectrolytes, including the effects of sodium chloride addition.²

$$\sigma_d = \frac{\epsilon k T \kappa}{e_o} \sinh\left(\frac{e_o \zeta}{2 k T}\right) \quad \text{where } \kappa = \sqrt{\frac{e_o N_A}{\epsilon k T} 2c} \quad (3)$$

A more complex model is required to explain the titration curves when PDADMAC is added to HPG–borate mixtures. Borate binding to HPG is expressed as the following equilibrium where $[B_c^-]$ is the concentration of free borate ions near the HPG, $[P]$ is the concentration of unoccupied borate binding sites on HPG, and $[BP^-]$ is the concentration of bound borate ions. For dilute mixtures of HPG and borate in the absence of other chemicals, $[B_c^-]$ approximately equals the average borate concentration in solution. The binding of borate to HPG has been described by eq 4 and the binding constants reported in the literature are 11 L/mol¹⁰ and 100 L/mol.¹²

$$K_1 = \frac{[BP^-]}{[B_c^-][P]} \quad (4)$$

The most important assumption in our model accounts for the depletion of free borate ions near a negatively charged interface and the corresponding enrichment of borate ions near a positive surface. This was accomplished through eq 5 which shows that when the local electrical potential HPG of the chain, ζ , is negative, the effective concentration of borate ions $[B_c^-]$ will be less than the average concentration in solution, $[B]$. The term γ is an adjustable parameter which was normally set at 3 – the sensitivity of model results to γ will be presented. We acknowledge similarities between eq 5 and the work of Leibler et al. who modeled the electrostatic retardation of borate binding by existing charges on the guar chain.¹⁵

$$[B_c^-] = [B] \exp\left(\frac{e_o \zeta \gamma}{k T}\right) \quad (5)$$

There are three contributions to net charge density on the SCD wall: σ_o the charge on the clean cell wall; σ_{HPG} the contribution of the borate groups bound to HPG; and, σ_{DAD} the charge associated with added cationic titrant (see eq 6). For a strong polyelectrolyte, the contributions of clean cell charge density and the adsorbed anionic polymer are constant; thus σ_{dl} in eq 2 was treated as a constant. By contrast, in HPG–borate titrations, σ_{HPG} may increase during the titration due to increased borate binding.

$$\sigma_d = \sigma_o + \sigma_{\text{HPG}} + \sigma_{\text{DAD}} \quad (6)$$

Equation 6 illustrates the three contributions to the net surface charge density of the surfaces of the SCD cell. The SCD reading for a clean cell is negative so σ_o , the initial cell charge density, was assumed to be constant and negative.

The contribution of the adsorbed HPG to charge density, σ_{HPG} , is given by eq 7 where Γ_{HPG} (mg/m²) is the coverage of adsorbed HPG, EW_{HPG} is the equivalent weight of HPG fully saturated with bound borate, $[P_T]$ is the total concentration of borate binding sites in the cell and F is the Faraday constant. We assume that Γ_{HPG} is constant, meaning that HPG does not desorb or adsorb during the titration. The term $[BP^-]/[P_T]$ is the fraction of occupied borate binding sites on HPG—thus we assuming that extent of borate binding in solution is the same of the HPG adsorbed on the cell wall. This is a serious approximation since ζ (see eq 5) near a borate binding site on HPG in solution will differ from ζ near the charged SCD cell surface.

$$\sigma_{\text{HPG}} = \frac{-\Gamma_{\text{HPG}}[BP^-]F}{EW_{\text{HPG}}[P_T]} \quad (7)$$

In the course of a titration, the cationic titrant (PDADMAC) binds to the HPG adsorbed on the HPG wall. It is unlikely that the amount of adsorbed HPG is constant during the titration. In the extreme as HPG–borate/PDADMAC approach neutrality, deposition of large complexes may occur. However, we are modeling the streaming potential which is sensitive to the composition at the shear plane. Thus, we are really assuming that HPG concentration at the shear plane is constant which is not too restrictive.

We assumed that all of the added PDADMAC is associated with HPG–borate so that the coverage of adsorbed PDADMAC, Γ_{DAD} , is given by eq 8, and the corresponding contribution to cell surface charge density is given by eq 9, where EW_{DAD} is the equivalent weight of PDADMAC (161 Da), and $C_{\text{DAD}}/C_{\text{HPG}}$ is the ratio of the total mass concentrations of PDADMAC to HPG in the cell. Note that during a titration, C_{DAD} increases from an initial value of 0, whereas C_{HPG} is constant.

$$\Gamma_{\text{DAD}} = \frac{C_{\text{DAD}}}{C_{\text{HPG}}} \Gamma_{\text{HPG}} \quad (8)$$

$$\sigma_{\text{DAD}} = \frac{\Gamma_{\text{DAD}}F}{EW_{\text{DAD}}} \quad (9)$$

The boric acid equilibrium is required to account for the influence of pH. Boric acid is a Lewis acid, forming the borate ion by reaction with hydroxyl. The borate formation constant (see eq 10 where $[B_T]$ is the total boron molarity), $K_o = 6.3 \times 10^4$ L/mol which corresponds to a pK_a of 9.2.

$$K_o = \frac{[B^-]}{([B_T] - [B^-])[OH^-]} \quad (10)$$

We employed borax ($\text{Na}_2\text{B}_4\text{O}_7 \cdot 10\text{H}_2\text{O}$) that adds two sodium ions for every four boron atoms. Thus, the following charge balance holds.

$$\frac{[B_T]}{2} + [H^+] = [OH^-] + [B^-] + [BP^-] \quad (11)$$

Equations 3–11 were solved numerically to give ζ as a function of the amount of added PDADMAC (C_{DAD}) using MathCAD 14. Most of the parameters have known values. The unknown parameters were the amount of adsorbed HPG, Γ_{HPG} , the electrostatic multiplier, γ , and α , the proportionality constant relating SCD signal to ζ potential.

Results

Polyelectrolyte Type. Figure 2 shows polyelectrolyte titration curves for three types of anionic polyelectrolytes titrated with

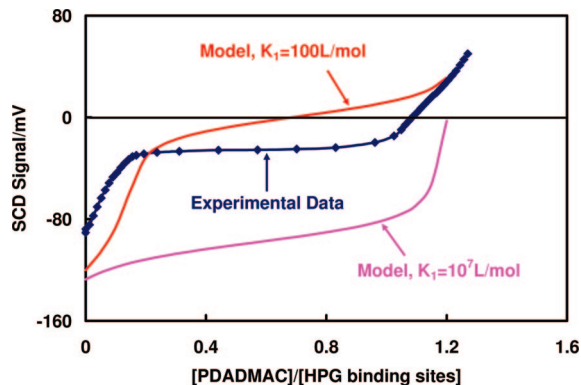


Figure 4. Comparing model and experimental polyelectrolyte titrations. The model parameters are as follows: $\gamma = 3$, $\sigma_o = -0.06$ C/m², $[\text{NaCl}] = 10$ mM, $[P_T] = 0.15$ mM, $[B_T] = 19$ mM, $\Gamma_{\text{HPG}} = 2$ mg/m², and $\alpha = 4$.

PDADMAC. The x -axis shows the volumes of PDADMAC added divided by the volume corresponding to 0 SCD signal. Potassium poly(vinyl sulfate), PVSK, is a strong polyelectrolyte which gives classic behavior. The SCD signal maintained a constant negative value to very near the end point.

The curve labeled PAA denotes the titration of poly(acrylic acid) at neutral pH where the degree of ionization is ~ 0.65 .¹⁶ The shape of the PAA titration is similar to PVSK and it has been long known that the polyelectrolyte titration gives good estimates of the degree of ionization of weak polyelectrolytes.¹⁷ For example, Phipps showed that potentiometric titration and polyelectrolyte titration gave the degree of ionization of polyethyleneimine as a function of pH.⁶ Thus, PAA and other standard weak polyelectrolytes do not undergo a significant change in the degree of ionization during the polyelectrolyte titration.

Finally, the nonideal HPG–borate titration curve in Figure 2 is the focus of this paper. The structure of HPG–borate is shown in Figure 3. This curve, and other examples to follow, show unusual features. Initially there is a rapid decrease in SCD signal followed by a long near constant section. Our explanation of the shape is that initially the HPG chain was not saturated with bound borate; however, the presence of cationic PDADMAC during the titration facilitates further borate binding. This hypothesis is built into our model described in the previous section.

Figure 4 compares the HPG–borate experimental curve with two simulated curves. The experimental SCD signals were divided by 4 to give values more typical of zeta potential measurements. In other words, α in eq 1 was assumed to be equal to 4. The x -axis for the experimental curve is the same as in Figure 2, whereas for simulated curves the x -axis is the equivalents of added PDADMAC divided by the total number of equivalents of borate binding sites on HPG.

The two simulated titrations differ in the borate binding constant, K_I in eq 4. The $K_I = 100$ L/mol curve shows the same features as the HPG–borate data. This is Jasinski's value for the binding constant.¹² By contrast, the simulated curve for the high binding constant closely resembles the PAA and PVSK curves in Figure 2. In this case the HPG is initially saturated with bound borate. The caption in Figure 4 gives the other model parameters. Of these, only γ and Γ_{HPG} were arbitrary—the sensitivity of the simulated curves to these arbitrary parameters will be shown at the end of this section.

Finally, we defined the end points of the simulated curves as the inflection points where the second derivative equals zero—see the Discussion section for justification. Thus, the end points for the simulated curves in Figure 4 correspond to the total amount of added titrant, being about 1.2 times the concentration

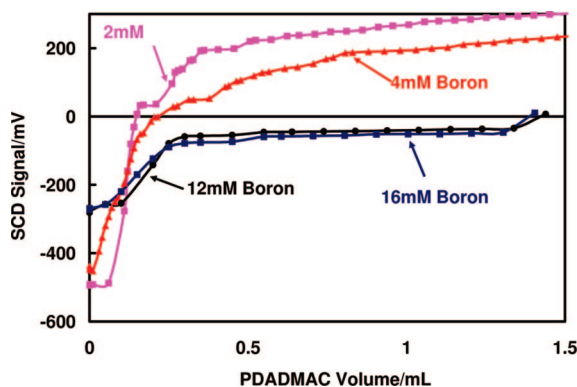


Figure 5. Influence of borate concentration on the titration of HPG-borate with PDADMAC.

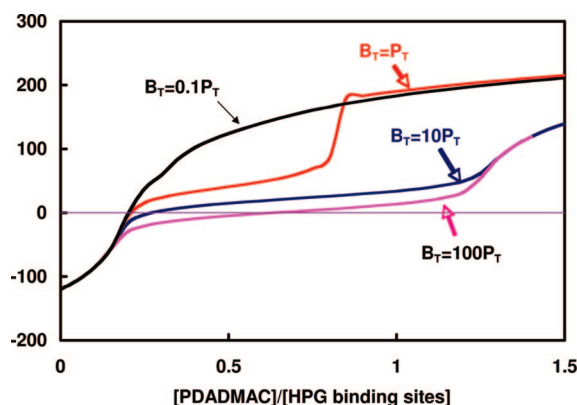


Figure 6. Simulating the influence of borate concentration. $K_1 = 100$ L/mol, with remaining parameters given in the caption of Figure 4.

of borate binding sites. The extra 20% reflects the initial charge on the cell wall (σ_0 in the model). We will show in following sections that the computed end points shift to the expected value of 1 when the concentration of adsorbed HPG (Γ_{HPG}) is increased.

Borate Concentration and pH. Borate serves two roles—when bound to HPG, borate is a source of charge and borate is a pH buffer. Figure 5 shows a series of titrations where the initial concentration of borax was varied. Note that we give the total concentration of boron species, which includes boric acid, free borate ion and borate bound to HPG. For high boron concentrations, the titrations were not sensitive to boron concentration, whereas lower borate concentrations influence the titrations. With very low borate in the cell, there is not enough to saturate the HPG chain and to keep the pH constant.

Figure 6 shows simulated titrations with varying borate concentrations. In this figure we express the total boron concentration, $[B_T]$, as a ratio to the total concentration of borate binding sites on HPG, $[P_T]$. Comparing the $B_T = 10P_T$ and $B_T = 100P_T$ curves showed that the end point was constant, whereas the higher borate concentration gave a small vertical shift toward more negative potentials. By contrast, when there was insufficient borate to saturate the HPG, the curves changed shape. The trends in Figure 6 show the main features of the experimental curves in Figure 5.

One might predict that at high total borate concentration, that the initial bound borate concentration should be high and that the shape of the polyelectrolyte titration should approach those of PAA or PVS. However, the negative surface potential near the clean cell lowers the amount of bound borate. The model accounts for this effect with eq 5. Consider, for example, the $B_T = 100P_T$ curve in Figure 6. The fraction of occupied borate

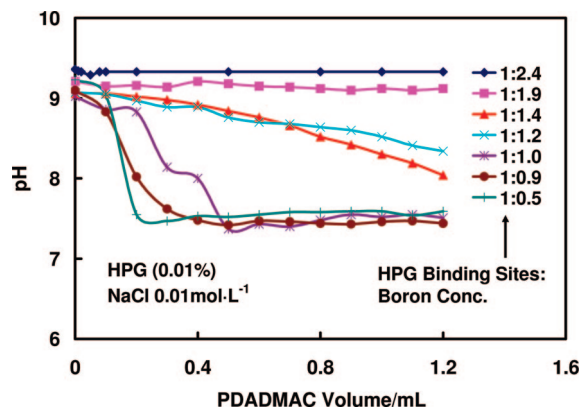


Figure 7. Evolution of pH during the titration of HPG-borate with PDADMAC.

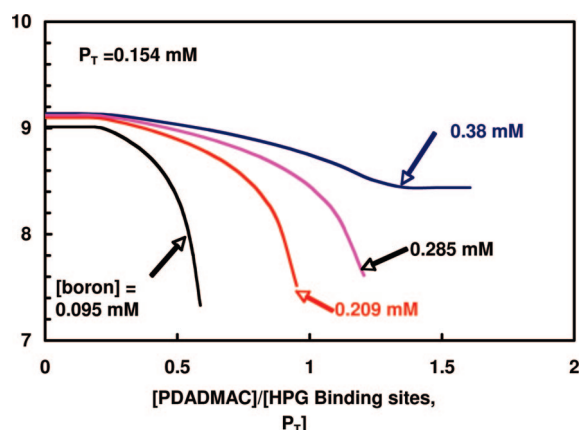


Figure 8. Simulating the influence of borate concentration on the evolution of pH during the titration of HPG-borate with PDADMAC. $K_1 = 100$ L/mol, with remaining parameters given in the caption of Figure 4.

binding sites on HPG is $6 \times 10^{-7} \sim 0$ before any PDADMAC is added. However, if we turn off the electrostatic influence on borate binding by setting $\gamma = 0$ in eq 5, the occupied fraction of borate binding sites is 0.43.

Borate binding lowers the pH because the bound ion can no longer participate as a buffer. Indeed, pH change measurement is one of the methods used to estimate borate binding constants.¹⁸ It was not possible to measure pH during a SCD titration; however, in independent experiments we monitored pH as a function of the quantity of PDADMAC added to HPG-borate mixtures. The results are summarized in Figure 7. The initial solutions were prepared with borax so that the initial pH approximately equaled the pK_a of 9.2. The boron concentrations are expressed as a fraction of the total concentration of borate binding sites on HPG. There was no pH change when very high boron concentrations were used (data not shown). The highest borate concentration in Figure 7 was 240% higher than the concentration of binding sites, so there was little pH change during the titration. By contrast, when the total boron concentrations were less than the concentration of binding sites, there was a substantial pH drop during the titration because PDADMAC addition induced most of the borate to bind to the HPG.

Our model was also capable of simulating the pH lowering during a titration. Figure 8 shows simulations at four initial boron concentrations. The model predicts the general features of the data in Figure 7. However, the detailed shapes of the pH evolution curves were sensitive to the assumed γ value - this will be shown in a later section.

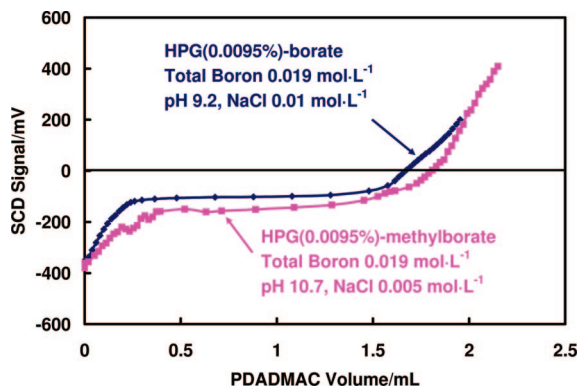


Figure 9. PDADMAC addition to HPG—methyl borate and to HPG—borate. The methylborate can only add once whereas borate can bind twice to give a cross-link.

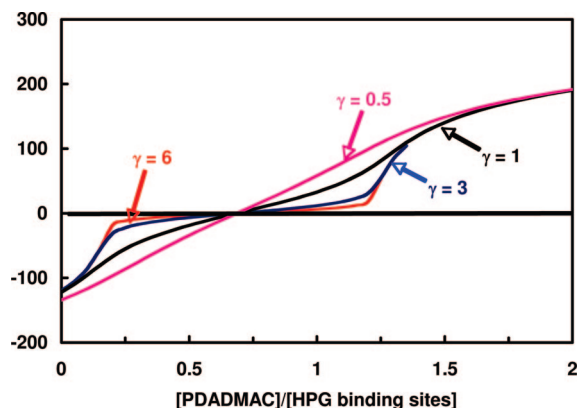


Figure 10. Influence of γ on the shape of the simulated polyelectrolyte titrations. $K_1 = 100$ L/mol, with remaining parameters given in the caption of Figure 4.

Borate Type. One of the complications of the HPG borate system is that a borate ion can bind twice to HPG giving a cross-link. We were concerned that the unusual SCD titration curves were some artifact of cross-linking. Several titrations were conducted in which boric acid was replaced with methylboronic acid. The alkyl boronate can only bind once, thus adding a charge to HPG without cross-linking. The two types of boric acids are compared in Figure 9. The most important conclusion is that the shapes of both curves are the same, showing that cross-link formation is not an important issue. A secondary point is that slightly more PDADMAC was required for the methylboronic solution. This suggests that with HPG—borate there were some cross-links because the HPG bound less borate than methyl borate.

Key Model Parameters. The major assumption in our model is that positive potential induced by PDADMAC increases the local borate concentration near the HPG which gives more binding. This assumption is implemented through eq 5 that contains the adjustable parameter γ . Figure 10 shows the influence of γ on the simulated titration curves. For γ values of 3 and greater the curves are not sensitive to γ and look similar to experimental curves. By contrast, the simulated curves for $\gamma = 1$ and $\gamma = 0.5$ were elongated showing little structure.

We also assumed that the amount of HPG adsorbed on the SCD detector wall, Γ_{HPG} , was constant throughout the titration. Figure 11 shows the influence of the amount of adsorbed HPG on the simulated titrations. For very high Γ_{HPG} values (10 and 200 mg/m²), the titration curves were independent of Γ_{HPG} and the end points corresponded to a dimensionless PDADMAC concentration equal to 1. This means the apparent end point was a measure of the total concentration of binding sites on

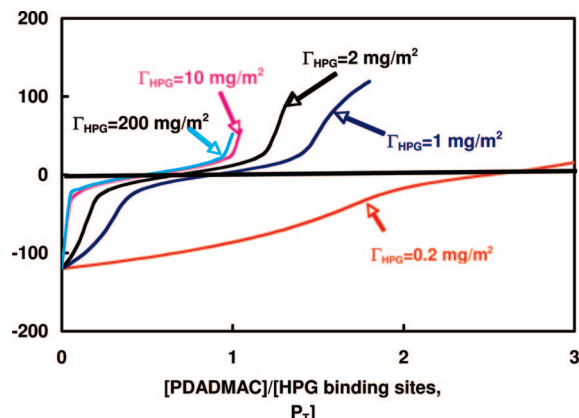


Figure 11. Influence of the assumed amount of adsorbed HPG on the shape of the simulated titrations. $K_1 = 100$ L/mol, with remaining parameters given in the caption of Figure 4.

HPG. However, the titration curves for the lower Γ_{HPG} values of 1 and 2 mg/m² were shifted to the right along the dimensionless PDADMAC axis. The shift in the end point to higher dimensionless PDADMAC concentrations reflects the larger contribution of initial charge density (clean cell before HPG is added, σ_0 in eq 6) to the consumption of cationic polymer. We propose that this sensitivity to clean cell charge density is exaggerated in the model because as HPG and PDADMAC adsorb, the shear plane will move out from the SCD wall, lowering the influence of σ_0 .

Discussion

Originally we performed colloid titrations on HPG—borate mixtures to measure the quantity of borate ions attached to HPG. Although the titrations were reproducible, their shapes were unusual and the end points corresponding to zero SCD signal seemed incorrect. The work herein was aimed at clarifying the criterion for choosing end points and to identify the meaning of the end point.

Examination of the experimental HPG—borate titration curves reveals that the PDADMAC volume corresponding to the end point is not distinct and does not correspond to a zero SCD signal. A better end point criterion is titrant volume where the second derivative of the curve is zero, although this was also indistinct in many cases with HPG—borate.

With the simulated titration curves, the ζ -potential corresponding to the end point could be positive or negative. If the binding constant, K_1 were high, the end point occurred when the SCD surface was still negatively charged whereas low K_1 values required a positively charged surface to saturate the HPG chain with bound borate.

The modeling suggests that the end point in our polyelectrolyte titrations gives a measure of the maximum number of borate binding sites on HPG. There is no consensus in the literature as to the identity of the binding sites on HPG ($[P_T]$ in the model). The three structural units on HPG (Figure 2) are galactose, bare mannose and mannose units supporting a galactose. The presence of the hydroxypropyl groups is another complication. The end points in our titrations correspond closely to the number of galactose units causing us to believe that most of the guar binding sites are on the galactose units. Ongoing work is attempting to prove this by other measurements of borate binding.

Our interest in HPG—borate behavior arises from its efficacy as a component of artificial tears.¹⁹ Previously, we showed that HPG—borate forms complexes with lysozyme, a cationic protein present in tear fluid.²⁰ The present work suggests that the

HPG–borate/lysozyme interaction is cooperative in that complexation may stimulate additional borate binding to HPG.

Finally, we propose that the polyelectrolyte titration of HPG–borate and HPG–methylborate illustrates polyelectrolyte behaviors that fall outside the conventional landscape of strong and weak polyelectrolytes. Specifically, the labile nature of the boronate binding causes the anionic charge density of HPG–borate to respond to small changes in local environment. In future work we will show that HPG–borate behaves like a conventional polyelectrolyte in that it can induce bridging flocculation. On the other hand, we will also show that unlike convention strong and weak anionic polyelectrolytes, HPG–guar does not complex with cationic surfactants. Therefore a picture is developing revealing that the interactions of labile HPG–borate with macromolecules and surfaces are more complicated than with conventional polyelectrolytes.

Conclusions

1. The polyelectrolyte titration does not measure the initial charge content of labile polyelectrolytes such as HPG–borate because the presence of cationic titrant facilitates further borate binding to HPG.

2. The polyelectrolyte titration can give a measure of the total concentration of borate binding sites on HPG.

3. End points for the HPG–borate polyelectrolyte titrations are not distinct and do not correspond to zero streaming current potential.

4. HPG binds slightly more methylboronic acid than borate ion because some of the borate ions occupy two sites on HPG, whereas methylboronic acid can bind only to one site.

5. The shapes of the polyelectrolyte titration curves and the pH changes during a titration were simulated by a model that accounts for electrostatic enhancement of borate binding to HPG in the presence of cationic PDADMAC.

Acknowledgment. This research was funded by the Natural Science and Engineering Research Council of Canada and by Alcon

Canada. The authors acknowledge Professor Bernard Cabane for useful discussions and Dr. Sheng Dai for first proposing our use of these titrations.

References and Notes

- (1) Terayama, H. *J. Polym. Sci.* **1952**, 8 (2), 243–253.
- (2) Pelton, R.; Cabane, B.; Cui, Y.; Ketelson, H. *Anal. Chem.* **2007**, 79, 8114–8117.
- (3) Kam, S. K.; Gregory, J. *Colloids Surf., A: Physicochem. Eng. Asp.* **1999**, 159 (1), 165–179.
- (4) Chen, J. H.; Heitmann, J. A.; Hubbe, M. A. *Colloids Surf. A: Physicochem. Eng. Asp.* **2003**, 223 (1–3), 215–230.
- (5) Bockenhoff, K.; Fischer, W. R. *Fresenius J. Anal. Chem.* **2001**, 371, 670–674.
- (6) Phipps, J. S. *Tappi J.* **1999**, 82 (8), 157–165.
- (7) Cheng, Y.; Brown, K. M.; Prud'homme, R. K. *Biomacromolecules* **2002**, 3, 456–461.
- (8) McNeil, M.; Albersheim, P. *Carbohydr. Res.* **1984**, 131 (1), 131–137.
- (9) Noble, O.; Taravel, F. R. *Carbohydr. Polym.* **1990**, 12 (3), 279–293.
- (10) Pezron, E.; Ricard, A.; Lafuma, F.; Audebert, R. *Macromolecules* **1988**, 21, 1121–1125.
- (11) Katchalsky, A.; Mazur, J.; Spitnik, P. *J. Polym. Sci.* **1957**, 23, 513–30.
- (12) Jasinski, R.; Redwine, D.; Rose, G. *J. Polym. Sci., Part B: Polym. Phys.* **1996**, 34, 1477–1488.
- (13) De Stefano, C.; Gianguzza, A.; Piazzese, D.; Sammartano, S. *J. Chem. Eng. Data* **2000**, 45, 876–881.
- (14) Walker, C. A.; Kirby, J. T.; Dentel, S. K. *J. Colloid Interface Sci.* **1996**, 182 (1), 71–81.
- (15) Leibler, L.; Pezron, E.; Pincus, P. A. *Polymer* **1988**, 29, 1105–1109.
- (16) Nagasawa, M.; Murase, T.; Kondo, K. *J. Phys. Chem.* **1965**, 69, 4005–4012.
- (17) Wassmer, K. H.; Schroeder, U.; Horn, D. *Makromol. Chem.—Macromol. Chem. Phys.* **1991**, 192, 553–565.
- (18) Springsteen, G.; Wang, B. H. *Tetrahedron* **2002**, 58, 5291–5300.
- (19) Christensen, M. T.; Cohen, S.; Rinehart, J.; Akers, F.; Pemberton, B.; Bloomenstein, M.; Leshner, M.; Kaplan, D.; Meadows, D.; Meuse, P.; Hearn, C.; Stein, J. M. *Curr. Eye Res.* **2004**, 28 (1), 55–62.
- (20) Lu, C.; Kostanski, L.; Ketelson, H.; Meadows, D.; Pelton, R. *Langmuir* **2005**, 21, 10032–10037.

MA801142R